Jefferson Lab PAC 44 Proposal

Determining the Pion Form Factor from Higher Q^2, High $-t$ Electroproduction Data

June 5, 2016

The pion has an important place in the study of the quark-gluon structure of hadrons due to its relatively simple $q\bar{q}$ valence structure. The charge form factor of the pion, $F_\pi(Q^2)$, is an essential element of the structure of the pion and is an object of great theoretical interest, especially at larger values of Q^2 where one can study nonperturbative dynamics of QCD while searching for a transition to the perturbative regime. This provides a benchmark for all models used to calculate the structure of hadrons. The last decade has seen a dramatic improvement in the understanding of pion electroproduction data. This has enabled us to optimize and link the previously approved E12-06-101 and E12-07-105 experiments, in order to extend these pion form factor data up to the highest possible momentum transfers achievable at a 12 GeV Jefferson Lab – $Q^2 \sim 8.5$ GeV^2. We request that the PAC confirm the high-impact status of such measurements and approve an additional 120 hours of beam time, to both obtain the needed statistics and enhance the validation for such a measurement.

G.M. Huber (Co-spokesperson)
University of Regina, Regina, SK, Canada

D. Gaskell (Co-spokesperson)
Physics Division, TJNAF, Newport News, VA

T.Horn (Co-spokesperson)
Catholic University of America, Washington, DC
Physics Division, TJNAF, Newport News, VA

Collaboration

S. Ali, M. Carmignotto, G. Kalicy, A. Mkrtchyan
Catholic University of America, Washington, DC, USA

T. Horn
Catholic University of America, Washington, DC and Physics Division, TJNAF, Newport News, VA, USA

J. Bericic, S. Covrig-Dusa, R. Ent, D. Gaskell, D. Higinbotham, M. Jones, T. Keppel, D. Mack,P. Nadel-Turonski, K. Park, B. Sawatzky, G.R. Smith, B. Wojtsekhowski, S. Wood
Physics Division, TJNAF, Newport News, VA, USA

Z. Ahmed, S. Basnet, G.M. Huber, W. Li, D. Paudyal, Z. Papandreou
University of Regina, Regina, SK, Canada

D. Abarms, D. Crabb, D. Day, D. Keller, D. Nguyen, D. Perera
University of Virginia, Charlottesville, VA, USA

B. Dongwi, M. Kohl, N. Kalantarians, A. Liyanage, J. Nazeer
Hampton University, Hampton, VA, USA

T. Brecelj, M. Mihovilovič, S. Širca, S. Štajner
Jožef Stefan Institute and University of Ljubljana, Slovenia

A. Asaturyan, H. Mkrtchyan, V. Tadevosyan
Alikhanyan National Science Laboratory, Yerevan, Armenia

W. Boeglin, P. Markowitz
Florida International University, Miami, FL, USA

I. Cloet, C.D. Roberts
Physics Division, Argonne National Laboratory, Argonne, IL, USA

D. Dutta, L. Ye
Mississippi State University, Starkville, MS, USA

G. Niculescu, I. Niculescu
James Madison University, Harrisonburg, VA, USA

D. Androic
University of Zagreb, Croatia

K. Aniol
California State University, Los Angeles, CA, USA

F. Benmokthar
Duquesne University, Pittsburgh, PA, USA

E.J. Brash
Christopher Newport University, Newport News, VA, USA

M. Bukhari
Jazan University, Saudi Arabia

D. Hamilton
University of Glasgow, Glasgow, Scotland, UK

C.E. Hyde
Old Dominion University, Norfolk, VA, USA

E. Kinney
University of Colorado, Boulder, CO, USA

C. Munoz-Camacho
Institut de Physique Nucleaire, Orsay, France

J. Roche
Ohio University, Athens, OH, USA

I. EXECUTIVE SUMMARY

The pion occupies a special role in nature [1]. It is the lightest quark system, with a single valence quark and a single valence antiquark. It is also the particle responsible for the long range character of the strong interaction that binds the atomic nucleus together. A general belief is that the rules governing the strong interaction are left-right, *i.e.* chirally, symmetric. If this were true, the pion would have no mass. The chiral symmetry of massless QCD is broken dynamically by quark-gluon interactions and explicitly by inclusion of light quark masses, giving the pion mass. The pion is thus seen as the key to confirm the mechanism that dynamically generates nearly all of the mass of hadrons and central to the effort to understand hadron structure.

This is evidenced by the proposed measurement of the pion form factor up to Q^2=6 GeV^2 (E12-06-101 [2]) being considered a flagship (and high-impact) goal of the upgraded 12 GeV Jefferson Lab. The last decade has seen a dramatic improvement in the understanding of pion electroproduction data [3–7]. This has now enabled revisiting the E12-06-101 experiment together with an approved "sister" experiment E12-07-105 [8] which aimed to probe conditions for factorization of deep exclusive measurements for charged pions to Q^2=9 GeV^2. An optimization of the kinematics of these two experiments (approved for 52 and 36 PAC days) now allows one to extend pion form factor data up to the highest possible momentum transfers achievable at a 12 GeV Jefferson Lab – Q^2=8.5 GeV^2. This would extend these high-impact measurements into the regime in which hard QCD's signatures will be quantitatively revealed. It would allow for confirming recent calculations tied to dynamical chiral symmetry breaking, and thus could contribute a major step forward towards our understanding of QCD.

The pion form factor, F_π, is not measured directly, but is determined indirectly via measurements of L/T-separated exclusive $p(e,e'\pi^+)n$ cross sections. To provide a meaningful measurement of the pion form factor up to the highest Q^2, several additional measurements are required. These include: (i) measurements of the exclusive π^-/π^+ ratio from deuterium, which is sensitive to isoscalar backgrounds that may complicate the extraction of F_π from electroproduction data, and (ii) measurements of π^+ electroproduction over a wide range of t at fixed Q^2 to confirm the model-independence of the extracted F_π values. This is a data-driven approach. Without such additional measurements, the high impact, high Q^2 F_π measurement would be much higher risk, open to the same questions and criticisms of interpretability [9] that have plagued the earlier Cornell measurements at similar Q^2[10].

We present here an optimized and linked run-plan for our two approved experiments, E12-06-101 and E12-07-105, that allows for the measurement of the pion form factor at the highest Q^2 achievable at a 12 GeV Jefferson Lab with minimal additional time. We request the PAC to confirm the high-impact status of such measurements. We also request PAC approval for an additional 120 hours of beam time, to both obtain the needed statistics and enhance the validation for such a Q^2=8.5 GeV^2 measurement.

II. THE RATIONALE FOR THE EXPERIMENT

A. Theoretical Motivation

Quantum Chromodynamics (QCD) is the strongly interacting part of the Standard Model. It is ultimately responsible for all of nuclear physics; and yet, almost fifty years after the discovery of gluons and quarks, we are only just beginning to understand how QCD builds the basic bricks of nuclei: neutrons and protons, and the pions that bind them together. QCD is characterized by two emergent phenomena: confinement and dynamical chiral symmetry breaking (DCSB), whose implications are truly extraordinary. These have far reaching consequences expressed in the character of the simplest mesons.

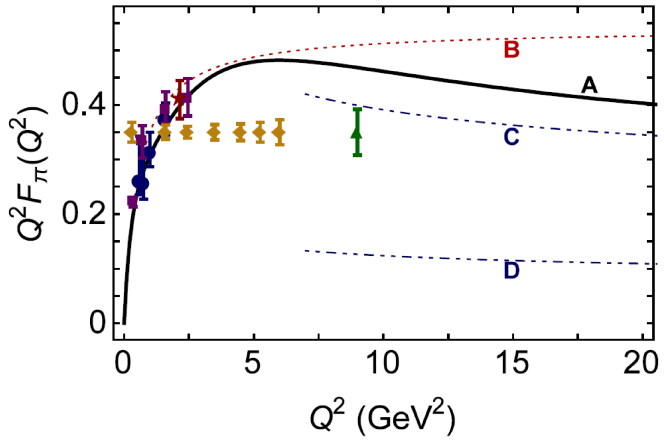

FIG. 1: Existing data (dark blue, purple) and projected uncertainties (yellow, green) for future data on the pion form factor. The solid curve (A) is the QCD-theory prediction bridging large and short distance scales. Curve B is set by the known long-distance scale, the pion radius. Curves C and D illustrate calculations based on a short-distance quark-gluon view. These studies were highlighted in the 2015 NSAC Long Range Plan [15].

Earlier 6 GeV Jefferson Lab measurements were at the beginning of a new era probing the internal pion structure. Measurements in Hall C by the F_π Collaboration [11, 12] confirmed that with a photon virtuality of 2.45 GeV^2 one is still far from the resolution region where the pion behaves like a simple quark/anti-quark pair, *i.e.* far from the "asymptotic" limit. However, this perception is based on the assumption that the asymptotic form of the pion's valence quark parton distribution amplitude (PDA) is valid at Q^2=2.45 GeV^2. The measured pion form factor is a factor of about three larger than the theoretical prediction. Modern calculations show that this factor could be explained by using a pion valence quark PDA evaluated at a scale appropriate to the experiment [13]. These calculations are closely tied to the DCSB, and thus confirming these calculations empirically would be a great step towards our understanding of

QCD.

One should expect dominance of hard contributions to the pion form factor for $Q^2 \geq$ 8 GeV^2 [14]. At about $Q^2 \sim$8 GeV^2, it is predicted that F_π will exhibit precisely the momentum-dependence from QCD, a power law behavior plus logarithmic corrections to scaling, but with the normalization fixed by a pion wave function whose dilation with respect to the asymptotic form is a definite signature of DCSB, which is a crucial feature of the standard model. Determination of the pion form factor at $Q^2 \sim$8 GeV^2 would extend elastic form factor data for the first time into the regime in which hard QCDs signatures will be quantitatively revealed. These studies illustrated in Fig. 1 were recently highlighted in the 2015 NSAC Long Range Plan [15].

B. Experimental Considerations

Experimental studies over the last decade have given us confidence in the reliability of the electroproduction method yielding the physical pion form factor. These studies included checking the consistency of the model used to extract the form factor from electroproduction data, by extracting the form factor at two values of t_{min} for fixed Q^2 and verifying that the pole diagram is the dominant contribution to the reaction mechanism. An example is illustrated in Fig. 2.

The resulting F_π values agree to 4% and do not depend on the t acceptance, which lends confidence in the applicability of the model to the kinematic regime of the data and the validity of the extracted F_π values. The dominance of the t-channel process in $\sigma_{\rm L}$ was verified through the charged pion longitudinal cross section ratios, $R_L = \sigma_L[n(e,e'\pi^-)p]/\sigma_L[p(e,e'\pi^+)n]$, obtained with a deuterium target. The data show that R_L approaches the pion charge ratio, consistent with pion-pole dominance.

This allows for an optimization of the kinematics of the two approved $p(e,e'\pi^+)n$ experiments to achieve a reliable F_π extraction up to the highest Q^2, along with similar experimental studies to confirm the results. The overall goals of the kinematics optimization of E12-06-101 and E12-07-105 were to:

- **Have a range of reliable F_π extractions from existing data to the highest possible Q^2.**
- **Validate the F_π extraction at the highest Q^2.**

Fig. 3 summarizes the optimized kinematics as a function of Q^2 and W (which may be viewed as another way to express $-t_{min}$) up to the highest possible value of Q^2. QCD background studies will be carried out at Q^2=1.6, 3.85, and 6.0 GeV^2.

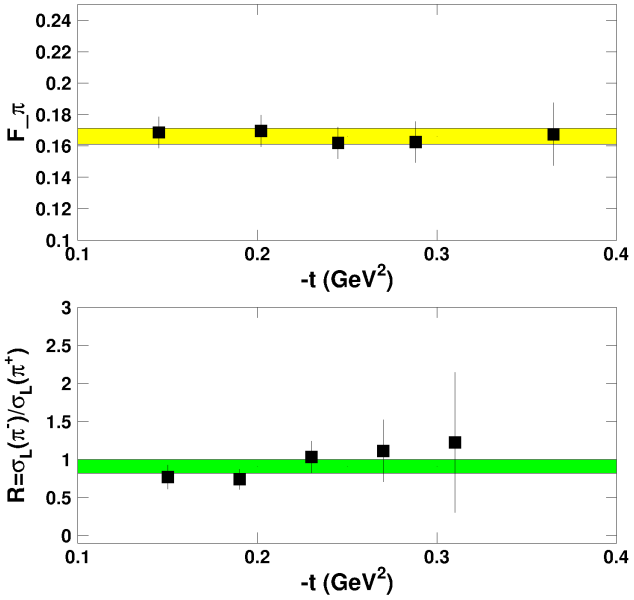

FIG. 2: **Upper panel:** Checking t- and model-dependence in the pion for factor extraction at a central value of Q^2=2.45 GeV^2 and center-of-mass energy W=2.22 GeV: the solid squares denote the F_π values for the case in which the model was fit to each point separately and the band shows the F_π value obtained from a fit to all points. The error bars and the error band include statistical and uncorrelated uncertainties. **Lower panel:** Checking the dominance of the t-channel process in $\sigma_{\rm L}$ through the charged-pion longitudinal cross section ratios at Q^2=2.45 GeV^2 and W=2.22 GeV. The cross-section ratios are close to unity and much larger than the ratios typically found for the transverse cross section, which is close to 1/4. This significant difference suggests pion pole dominance in the longitudinal cross sections (and parton model dominance in the transverse). The error bars include statistical and uncorrelated uncertainties, and the (green) band denotes the uncertainty of a constant fit to all data points.

III. DETERMINING F$_\pi$ FROM ELECTROPRODUCTION DATA

Due to the extensive experience gained during our previous F_π measurements in Hall C [12], as well as lessons learned from previous work at Cornell [10] and DESY [16], many of the experimental difficulties in extracting the pion form factor at higher Q^2 are well understood. This section discusses the issues of greatest relevance.

A. The role of the proton's pion cloud

Experimentally, pion elastic form factor measurements at higher Q^2 are made indirectly, using exclusive pion electroproduction, $p(e,e'\pi^+)n$, to gain access to the proton's "pion cloud".

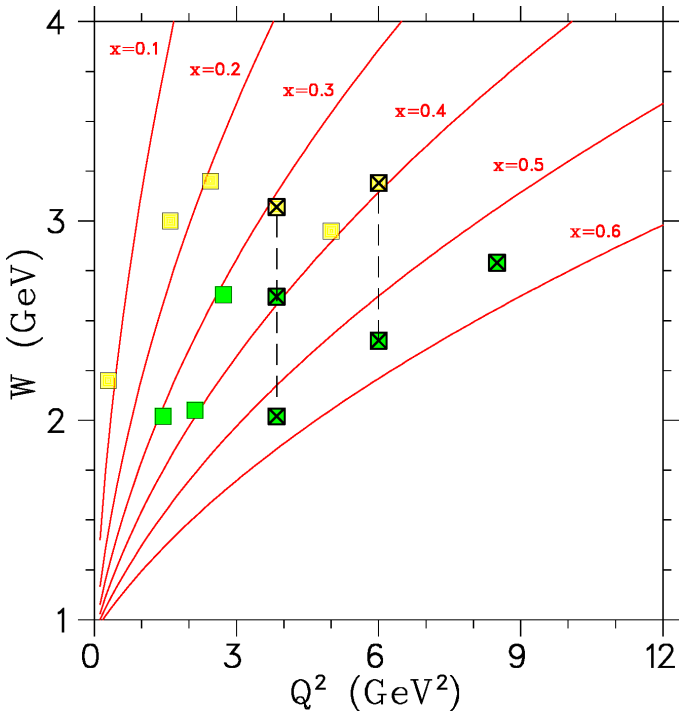

FIG. 3: Updated W versus Q^2 settings planned for the F_π experiment (yellow squares) and the "Pion Scaling" experiment E12-07-105 (green squares). The points instrumental in the higher Q^2 F_π extraction are indicated with 'X'. The red lines indicate fixed x values from 0.1 to 0.6. The dashed lines denote scans in t at fixed Q^2, which will be used to evaluate the dependence of the F_π extraction on t as shown in Fig. 2.

At values of t approaching the pion mass squared (the so called t-pole), the longitudinal response function becomes approximately proportional to the square of the charged pion form factor

$$\sigma_L \approx \frac{-tQ^2}{(t-M_\pi^2)^2} g_{\pi NN}^2(t) F_\pi^2(Q^2,t). \tag{1}$$

Here, the factor $g_{\pi NN}(t)$ comes from the πNN vertex and represents the probability amplitude to have a virtual charged π meson inside the nucleon at a given t.

The experimental determination of the pion form factor from low $-t$ electroproduction data, the interpretability issues which affected the high Q^2 data from Cornell, and how these issues may be controlled, are explained at length in our 2006 proposal [2]. To briefly summarize, L/T-separated $p(e,e'\pi^+)n$ cross sections versus t over some range of Q^2 and W are the actual observables measured by the experiment, and the extraction of the pion form factor from these data is via a phenomenological model. Our 4–6 GeV measurements in Hall C have shown this approach to yield reliable F_π values from forward kinematics data [12]. Since the VGL Regge model [17] is able, without fitted parameters, to provide a good description of both π^+ and π^-

photoproduction data, and of $\sigma_{\rm L}$ electroproduction data over a range in W, t, and Q^2, we have used it to extract pion form factor values from the JLab $\sigma_{\rm L}$ data up to a maximum Q^2 value of 2.45 GeV^2. Ideally, one would like to have a variety of reliable electroproduction models to choose from, so that the model dependence of the extracted F_π values can be better understood. Since it remains our intent to publish the $\sigma_{\rm L}$ values obtained by our experiment, other F_π values may result when better models become available in the future.

For this proposal, it is important to note that for W above the resonance region, the t-channel pion pole process dominates $\sigma_{\rm L}$ for small $-t$ and contributes unequally to the L, T, TT, and LT responses. Competing non-pole production processes also contribute to $\sigma_{\rm L}$, but they are small in forward kinematics (*i.e.* $-t_{min} < 0.2$ GeV^2) and do not have a pole at $t = m_\pi^2$. To maximize the contribution of the t-channel process, as well as separate it from the others which tend to disguise its effect, one measures at a low $-t$ in parallel and near-parallel kinematics, and performs a response function separation. This is the approach that will be followed in our approved E12-06-101 experiment. The $Q^2 = 6$ GeV^2 upper bound of these measurements is partly dictated by the requirement $-t_{min}$ <0.2 GeV^2, needed to assure the dominance of the pion pole process to $\sigma_{\rm L}$.

However, the 11 GeV electron beam energy and Hall C equipment allow reliable L/T-separations within a reasonable amount of beam-time up to about Q^2 ∼9 GeV^2, the approved high Q^2 point in our experiment E12-07-105. If one can experimentally show independence of t, this would allow one to measure F_π in Hall C to significantly higher than Q^2=6.0 GeV^2. Here, we propose such a data-driven approach, to acquire the additional data which will aid understanding the non-pion pole contributions to $\sigma_{\rm L}$ at higher $-t$.

The goals of the experimental studies proposed here are to:

1. Optimize the kinematics of E12-06-101 and E12-07-105 to allow for acquiring high quality Q^2=8.5 GeV^2 L/T-separated $p(e,e'\pi^+)n$ data with the SHMS+HMS in Hall C.

2. Acquire the vital validation data needed to constrain the non-pion pole backgrounds to $\sigma_{\rm L}$ at higher $-t$ and enable F_π to be reliably extracted.

B. Test F_π extractions at same Q^2 but different $-t_{min}$

In our two previous experiments, E93-021 (Fpi-1) and E01-004 (Fpi-2), we acquired $p(e,e'\pi^+)n$ L/T-separated $Q^2 = 1.6$ GeV^2 data at different distances from the pion pole and compared the resulting F_π values [12]. Fpi-1 measurements were obtained at $W = 1.95$ GeV, $-t_{min}$ =0.152 GeV^2, while the Fpi-2 data were obtained 35% closer to the pole, at $W = 2.22$ GeV $-t_{min}$ =0.093 GeV^2. The VGL model incorporates a monopole form for the $\pi\pi\gamma$ and $\rho\pi\gamma$ form factors:

$$F_{\pi,\rho}(Q^2) = [1 + Q^2/\Lambda^2_{\pi,\rho}]^{-1}. \quad (2)$$

Apart from the $\pi\pi\gamma$ and $\rho\pi\gamma$ form factors, the VGL model is parameter free, as the coupling constants at the vertices (such as $g_{\rho\pi\gamma}$) are well determined by precise studies and analyses in the resonance region. The optimal value of Λ_π^2 is determined from a fit to each set of $\sigma_{\rm L}$ data (it is insensitive to Λ_ρ^2), yielding the empirical F_π values. A comparison of the F_π values extracted from the data sets in this manner allows for a direct test of the theoretical model dependence. The two F_π values extracted from Q^2=1.6 GeV^2 data at W=1.95, 2.22 GeV are in excellent agreement (4% difference, well within errors), suggesting only a small uncertainty due to fitting the VGL model to the $\sigma_{\rm L}$ data. This technique is not specifically wedded to the VGL model, in principle any model used to extract F_π from electroproduction data should pass this test.

As part of the validation procedure for the extraction of F_π from higher $-t$ Q^2=8.5 GeV^2 data, we will perform several similar tests as part of the optimized E12-06-101 and E12-07-105. At Q^2=3.85 GeV^2, we will acquire three sets of L/T-separated data, at $-t$ =0.120 GeV^2, W=3.07 GeV; $-t$=0.208 GeV^2, W=2.62 GeV; and $-t$=0.487 GeV^2, W=2.02 GeV. We will extract F_π from all three sets of data and see if they are consistent. A second test will be performed at higher Q^2=6.00 GeV^2, at $-t$=0.214 GeV^2, W=3.19; and $-t$=0.530 GeV^2, W=2.40 GeV. If the two F_π values extracted from these higher Q^2 data are consistent, then we will have very good reason to believe that our extraction of F_π from Q^2=8.5 GeV^2, $-t$=0.550 GeV^2 data is reliable. If they are not initially consistent, then the redundant scans are absolutely vital for understanding the nature of the non-pole backgrounds, so that F_π can ultimately be extracted from these data.

C. The sensitivity of π^-/π^+ measurements to non-pion pole backgrounds

An important tool to infer the presence of isoscalar backgrounds to $\sigma_{\rm L}$ is the measurement of the ratio

$$R_L = \frac{\sigma(n(e,e'\pi^-)p)}{\sigma(p(e,e'\pi^+)n))} = \frac{|A_v - A_s|^2}{|A_v + A_s|^2}$$

using a liquid deuterium target. The t-channel pion-pole diagram is a purely isovector process, and so at small $-t$, R_L should be near unity. Isoscalar backgrounds are expected to be suppressed by the $\sigma_{\rm L}$ response function extraction. Nonetheless, if they are present to any significant degree, they will result in a dilution of the ratio. R_L data were acquired as part of our Fpi-1, Fpi-2 experiments, and proved themselves to be extremely valuable in two ways:

1. In Fpi-2, the extraction of F_π from our Q^2=1.6, 2.45 GeV^2, W=2.2 GeV data via the VGL model encountered no significant difficulties. We estimated only a small model dependence in the F_π results, and the R_L data confirmed that isoscalar backgrounds in these data were small.

2. In Fpi-1, we encountered inconsistencies when extracting F_π from our Q^2=0.6-1.6 GeV^2, W=1.95 GeV data. We were required to apply corrections to the VGL model and assess a larger model dependence. R_L data not only confirmed the presence of isoscalar contributions to our higher $-t$ data, but they also also indicated that these contributions are much smaller near $-t_{min}$, validating the approach we followed to extract F_π from these data.

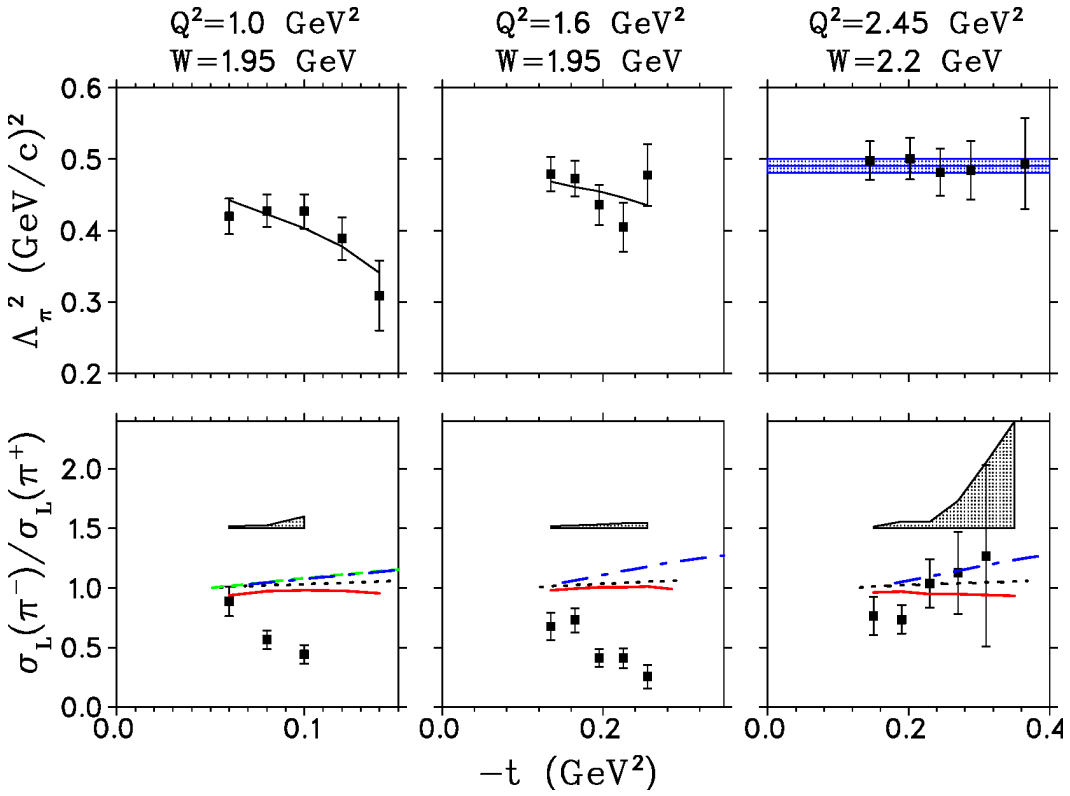

FIG. 4: **Top Row:** Consistency check for the extraction of F_π from Fpi-1, Fpi-2 data by plotting the value of Λ_π^2 determined from the fit of the VGL model to each t-bin of $\sigma_{\rm L}$ data. If the Λ_π^2 values display no t-dependence, no further corrections are needed to extract F_π from the data, as indicated in the right-most W=2.2 GeV panel. The left and center panels required additional corrections and model-dependence, as discussed in Ref. [12]. **Bottom Row:** R_L data compared to a variety of models (e.g. dotted black [17]; dot-dashed blue [18]). R_L ~0.8, near $-t_{\rm min}$ at each Q^2 setting, corresponding to $A_S/A_V = 6\%$ under the not necessarily realistic assumption that the isoscalar and isovector amplitudes are real. At higher $-t$, the W=1.95 GeV R_L data deviate strongly from both this ratio and the expectations of various models, indicating the presence of isoscalar contributions to $\sigma_{\rm L}$. For more details see Ref. [3].

The comparison of these two sets of results is shown in more detail Fig. 4. The top row shows the values of Λ_π^2 determined from fits of the VGL model to our $\sigma_{\rm L}$ data. The bottom row shows the R_L data for the same settings. In the right column are our Q^2=2.45 GeV^2, W=2.2

GeV data, where neither the Λ_π^2 nor R_L values display any statistically significant t-dependence, indicating the dominance of the t-channel diagram across the full range of the data. In this case, the R_L data confirmed that it was possible to extract F_π from the $\sigma_{\rm L}$ data without further corrections. The situation is somewhat different for the Q^2=1.0, 1.6 GeV^2 data at W=1.95 GeV (left and center columns). Λ_π^2 drops at higher $-t$ due to additional contributions to $\sigma_{\rm L}$ not taken into account by the VGL model. The R_L ~0.8 values near $-t_{min}$ indicate that the non-pole contributions are small there, but the dropping R_L values indicate they grow rapidly at higher $-t$. In these cases, the R_L data validate the approach we used to extract F_π from these data, which relied on the assumption that non-pole contributions were smallest at $-t_{min}$. The bottom line is that R_L tests can and must be performed to indicate where the longitudinal data are dominated by the t-channel process. This lends confidence in the F_π values extracted from the experimental data.

Unfortunately, it is experimentally expensive to carry out these π^-/π^+ measurements. Due to the negative polarity of the pion spectrometer, electron singles rates are high and it is usually necessary to lower the beam current from about 70 μA to 10-15 μA to maintain the excellent tracking and particle identification needed for reliable L/T-separations. We have investigated whether it would be feasible to acquire π^-/π^+ measurements at Q^2=8.5 GeV^2, W=2.79 GeV, $-t_{min}$=0.550 GeV^2, but this would take a prohibitive 3600 PAC-hrs of beam. Therefore, we propose to perform this test at Q^2=6.0 GeV^2, W=2.40 GeV, $-t_{min}$=0.530 GeV^2, where the pion production cross sections and electron singles rates are projected to be much more favorable. Since the $-t$ and Q^2 values are similar, and our previous R_L measurements indicate only a weak Q^2-dependence at fixed $-t$, we expect this measurement to provide vital information on any non-pole backgrounds contributing to $\sigma_{\rm L}$ at Q^2=8.5 GeV^2.

The previously approved E12-06-101 and E12-07-105 included high statistics π^-/π^+ measurements at low $-t$ at Q^2=1.6, 3.50 GeV^2, and limited statistics π^-/π^+ measurements at Q^2=2.12, 5.50 GeV^2. We have reorganized our planned settings, to enable additional additional π^-/π^+ data to be acquired at intermediate $-t_{min}$, so that the evolution of the non-pole backgrounds versus $-t$ can be better understood. The revised π^-/π^+ plan includes two scans at Q^2=3.85 GeV^2: W=3.07 GeV, $-t_{min}$ =0.120 GeV^{2}and W=2.62 GeV, $-t_{min}$ =0.208 GeV^2, and higher statistics for the previously approved Q^2=2.12 GeV^2 measurement. These, together with the π^-/π^+ setting at Q^2=6.0 GeV^2 mentioned above, are vital to determine the presence of non-pole backgrounds if F_π is to be reliably extracted from higher $-t$ electroproduction data.

IV. COMPREHENSIVE KINEMATICS PLAN

The optimized kinematics for both E12-06-101 and E12-07-105 are presented graphically in Fig. 3 and in detail in Tables I, II, and III. We have saved some beamtime by combining and reorganizing settings between the two experiments, so that the additional time needed for

TABLE I: Optimized settings for the E12-06-101 (Fpi-12) experiment. The scattered electron will be detected in the HMS and the pion in the SHMS. LH+, LD+, LD- indicate the combination of cryotarget type and SHMS (pion) polarity. Hours per setting include both full and dummy target data taking, as well as 4 hours of overhead. The settings in *blue italics* are used for both the pion form factor and pion scaling studies.

Q^2	W	x	$-t_{min}$	Type	E_e	Gradient	ϵ	θ_q	$\theta_{\pi q}$	Hrs
0.30	2.20	0.070	0.005	LH+	2.8	1.37	0.341	5.71	0, +2, +4^o	12.8
					3.7	1.82	0.657	8.33	-2, 0, +2, +4^o	15.7
					4.2	1.37	0.747	9.11	-2, 0, +2, +4^o	15.7
1.60	3.00	0.165	0.029	LH+	6.7	Std.	0.408	6.36	0, +2^o	9.9
					8.8	Std.	0.689	8.70	-2, 0, +2^o	12.8
					11.0	Std.	0.817	9.91	-2, 0, +2^o	12.8
1.60	3.00	0.165	0.029	LD+	6.7	Std.	0.408	6.36	0, +2^o	9.9
					11.0	Std.	0.817	9.91	-2, 0, +2^o	12.8
1.60	3.00	0.165	0.029	LD-	6.7	Std.	0.408	6.36	0, +2^o	18.7
					11.0	Std.	0.817	9.91	-2, 0, +2^o	12.8
2.45	3.20	0.208	0.048	LH+	8.0	1.96	0.383	6.26	0, +2^o	9.9
					8.8	Std.	0.505	7.30	-1.8, 0, +2^o	12.8
					11.0	Std.	0.709	9.03	-2, 0, +2^o	12.8
3.85	*3.07*	*0.311*	*0.120*	*LH+*	*8.0*	*1.96*	*0.301*	*6.53*	*-1.03, 0, +2^o*	*33.5*
					8.8	*Std.*	*0.436*	*7.97*	*-2, 0, +2^o*	*18.2*
					9.9	*1.96*	*0.572*	*9.31*	*-2, 0, +2^o*	*13.3*
					11.0	*Std.*	*0.666*	*10.27*	*-2, 0, +2^o*	*12.8*
3.85	3.07	0.311	0.120	LD+	8.0	1.96	0.301	6.53	-1.03, 0, +2^o	33.5
					11.0	Std.	0.666	10.27	-2, 0, +2^o	12.8
3.85	3.07	0.311	0.120	LD-	8.0	1.96	0.301	6.53	0, +2^o	118.8
					11.0	Std.	0.666	10.27	-2, 0, +2^o	12.8
5.00	*2.95*	*0.390*	*0.209*	*LH+*	*8.0*	*1.96*	*0.238*	*6.35*	*0, +2^o*	*74.5*
					9.9	*1.96*	*0.530*	*9.76*	*-2, 0, +2^o*	*41.1*
					11.0	*Std.*	*0.633*	*10.88*	*-2, 0, +2^o*	*27.0*
6.00	*3.19*	*0.392*	*0.214*	*LH+*	*9.2*	*1.82*	*0.184*	*5.13*	*0.37, +2^o*	*182.2*
					9.9	*1.96*	*0.304*	*6.64*	*0, +2^o*	*80.6*
					11.0	*Std.*	*0.452*	*8.22*	*-2, 0, +2^o*	*71.9*
Calibrations										80.0
Beam Energy Changes										72.0
Total Hours (100% efficiency)										1054.4
PAC35 Approved Hours (100% efficiency)										1248.0
Time Saved: 1248-1054.4 hrs (100% efficiency)										-193.6

the higher Q^2 F_π study and reliability tests is minimized. A detailed running-time breakdown in comparison to our previous PAC approval is shown in Table IV.

In the optimization of the two experiments we took into account the comments of the PAC30 [19] and PAC32 [20] written reports. In particular, We optimized the settings from E12-06-101 and E12-07-105 in the following way:

- Justification of the beam time for the highest x/Q^2 point (PAC32):

TABLE II: Optimized settings for the E12-07-105 (Pion Scaling) experiment, as per Table I. The setting in **bold face** is for the pion form factor extraction at high Q^2. The settings in *blue italics* are for validating the possibility of pion form factor extractions at high t at Q^2=2.12 and 3.85 GeV^2.

Q^2	W	x	$-t_{min}$	Type	E_e	Gradient	ϵ	θ_q	$\theta_{\pi q}$	Hrs
1.45	2.02	0.312	0.114	LH+	3.7	1.82	0.523	13.94	-2, 0, +2^o	12.8
					6.7	Std.	0.880	20.17	-2, 0, +2^o	12.8
2.73	2.63	0.311	0.118	LH+	6.7	Std.	0.513	10.30	-2, 0, +2^o	12.8
					11.0	Std.	0.845	14.58	-2, 0, +2^o	12.8
2.12	2.05	0.390	0.195	LH+	4.5	Std.	0.559	14.92	-2, 0, +2^o	12.8
					8.8	Std.	0.907	21.44	-2, 0, +2^o	12.8
2.12	*2.05*	*0.390*	*0.195*	*LD+*	*4.5*	*Std.*	*0.559*	*14.92*	*-2, 0, +2^o*	*12.8*
					8.8	*Std.*	*0.907*	*21.44*	*-2, 0, +2^o*	*12.8*
2.12	*2.05*	*0.390*	*0.195*	*LD-*	*4.5*	*Std.*	*0.559*	*14.92*	*-2, 0, +2^o*	*12.8*
					8.8	*Std.*	*0.907*	*21.44*	*-2, 0, +2^o*	*12.8*
3.85	2.62	0.392	0.208	LH+	6.7	Std.	0.360	8.94	-2, 0, +2^o	30.0
					11.0	Std.	0.799	14.58	-2, 0, +2^o	12.8
3.85	*2.62*	*0.392*	*0.208*	*LD+*	*6.7*	*Std.*	*0.360*	*8.94*	*-2, 0, +2^o*	*30.0*
					11.0	*Std.*	*0.799*	*14.58*	*-2, 0, +2^o*	*12.8*
3.85	*2.62*	*0.392*	*0.208*	*LD-*	*6.7*	*Std.*	*0.360*	*8.94*	*-2, 0, +2^o*	*99.8*
					11.0	*Std.*	*0.799*	*14.58*	*-2, 0, +2^o*	*12.8*
3.85	2.02	0.546	0.487	LH+	6.0	1.96	0.582	17.41	-2, 0, +2^o	12.8
					11.0	Std.	0.898	21.92	-2, 0, +2^o	12.8
6.00	2.40	0.551	0.530	LH+	8.0	1.96	0.449	11.26	-2, 0, +2^o	48.5
					11.0	Std.	0.738	15.31	-2, 0, +2^o	18.4
8.50	**2.79**	**0.552**	**0.550**	**LH+**	**9.2**	**1.82**	**0.156**	**5.52**	**0^o**	**388.0**
					11.0	**Std.**	**0.430**	**9.36**	**0^o**	**108.5**
Calibrations										48.0
Beam Energy Changes										72.0
Total Hours (100% efficiency)										1035.3
PAC38 Approved Hours (100% efficiency)										864.0
Time saved: 1035.3-864-193.6 (Table I) hrs (100% efficiency)										-22.3

TABLE III: Additional settings required to validate the F_π extraction at Q^2=8.5 GeV^2

.

Q^2	W	x	$-t_{min}$	Type	E_e	Gradient	ϵ	θ_q	$\theta_{\pi q}$	Hrs
6.00	2.40	0.551	0.530	LD+	8.0	1.96	0.449	11.26	-2, 0, +2^o	48.5
					11.0	Std.	0.738	15.31	-2, 0, +2^o	18.4
6.00	2.40	0.551	0.530	LD-	8.0	1.96	0.449	11.26	-2, 0, +2^o	48.5
					11.0	Std.	0.738	15.21	-2, 0, +2^o	18.4
Calibrations										8.0
Beam Energy Changes										0.0
Total Hours (100% efficiency)										141.8

This Beam Request: 141.8-22.3 hrs	119.5

TABLE IV: Detailed breakdown of optimized run times compared to PAC35 and PAC38 approvals.

Q^2	W	x	$-t_{min}$	Type	PAC35	New Plan	Difference (New-PAC35)
E12-06-101 (Fpi-12)							
0.30	2.20	0.070	0.005	LH+	36	44.2	
1.60	3.00	0.165	0.029	LH+	36	35.5	
				LD+	20	22.7	
				LD-	25	31.5	
2.45	3.20	0.208	0.048	LH+	57	35.5	-4.6
3.50	3.10	0.286	0.099	LH+	48		
				LD+	32		
				LD-	157		
3.85	3.07	0.311	0.120	LH+		77.8	
				LD+		46.3	
				LD-		131.6	18.7
4.46	3.25	0.315	0.124	LH+	122		
5.25	3.20	0.359	0.171	LH+	216		
5.00	2.95	0.390	0.209	LH+		142.6	-195.4
6.00	3.19	0.392	0.214	LH+	345	334.7	-10.3

Q^2	W	x	$-t_{min}$	Type	PAC38	New Plan	Difference (New-PAC38)
E12-07-105 (Pion Scaling)							
1.45	2.02	0.312	0.114	LH+	9.4	25.6	
2.73	2.63	0.311	0.118	LH+	14.4	25.6	
4.00	3.12	0.311	0.120	LH+	14.1		12.3
2.12	2.05	0.390	0.195	LH+	9.6	25.6	
				LD+		25.6	
				LD-	9.6	25.6	57.6
3.85	2.62	0.392	0.208	LH+		42.8	
				LD+		42.8	
				LD-		112.6	
4.00	2.67	0.390	0.206	LH+	23.5		
				LD+			
				LD-	23.5		151.2
5.50	3.08	0.390	0.210	LH+	38.6		
				LD+			
				LD-	38.6		-77.2
3.85	2.02	0.546	0.487	LH+		25.6	
4.00	2.04	0.549	0.498	LH+	14.6		11.0
6.00	2.40	0.551	0.530	LH+		66.9	
6.60	2.51	0.549	0.530	LH+	152.8		-85.9
8.50	2.79	0.552	0.550	LH+		496.5	
9.10	2.89	0.549	0.545	LH+	416.4		80.1

Q^2	W	x	$-t_{min}$	Type	PAC35/38	New Plan	Difference (New-PAC35/38)
Additional Settings (Validation of F_π extraction at high Q^2)							
6.00	2.40	0.551	0.530	LD+		66.9	
				LD-		66.9	
							133.8

  - We moved the previous E12-07-105 point at Q^2=9.1 GeV^2 to Q^2=8.5 GeV^2 to extend pion form factor data to the highest possible Q^2 at the 12 GeV Jefferson Lab. This setting benefits from reduced uncertainties due to higher rate and more favorable $1/\Delta\epsilon$ error magnification. Some beam time was added for the higher statistics needed for the F_π extraction. Overall, the potential physics outcome fully justifies the large beam time requirement.
  - The Q^2=8.5 GeV^2 setting requires non-standard beam energies. If only standard beam energies are required, our run plan can be adjusted to a highest Q^2 of 8.3 GeV^2.

- Optimization between the two experiments (PAC32):

  - To achieve better overlap between the two experiments, we moved the Q^2=6.6 GeV^2 point from E12-07-105 to 6.0 GeV^2. Together with the E12-06-101 point at Q^2=6.0 GeV^2, this provides a suitable range from $-t$=0.21 to $-t$=0.80 GeV^2, to verify the reliability of F_π extraction at higher Q^2 and higher $-t$.
  - The approved intermediate Q^2 points from both E12-06-101 and E12-07-105 were rearranged to a common Q^2=3.85 GeV^2, to better investigate the t-dependence of the reaction. These points also included measurements of the π^+/π^- ratio, which will allow us to test for QCD backgrounds in the F_π extraction.

- Optimization of the schedule (PAC30):

  - Considerable time was saved by eliminating points at Q^2=4.46 GeV^2 (E12-06-101) and Q^2=5.50 GeV^2 (E12-07-105). The Q^2=5.25 GeV^2 point of E12-06-101 was moved to Q^2=5.00 GeV^2, so that it may serve double-duty as part of the x=0.39 scan of E12-07-105.
  - Where possible, we revised all settings to minimize the number of settings requiring special linac gradients, and reduce the most forward SHMS angle requirements. Rates are based on a SIMC Monte Carlo simulation using the VR cross-section model [18], with all experimental acceptance and missing mass cuts applied.

- Use of a 10-cm long target to reduce the beam current (PAC30):

  - We have increased the target cell length from 8 cm to 10 cm. This allows for a reduction of the maximum beam current from 85 μA (with 8 cm target as assumed for PAC35/38) to 70 μA.

– Precise L/T separations require a systematic understanding of the spectrometer acceptance over the extended target length. The largest target is with the HMS spectrometer at 57 degrees. We have added 8 hours to allow for detailed checks of the acceptance in Table III. Further details on the extended target acceptance studies can be found in Sec. A.

To ensure the reliability of the potentially high impact Q^2=8.5 GeV^2 pion form factor measurement, we added some additional studies of the possible non-pole contributions in Table III. Specifically, a new set of π^-/π^+ measurements was added at Q^2=6.0 GeV^2, at comparable $-t$ to the Q^2=8.5 GeV^2 /fpi/ extraction point. Since our previous R_L measurements indicate only a weak Q^2-dependence at fixed $-t$, we expect this measurement to provide vital information on the non-pole backgrounds contributing to $\sigma_{\rm L}$ at Q^2=8.5 GeV^2.

Combining kinematic points effectively and optimizing kinematics resulted in significant beam time savings. The total extra time required to allow for an extraction of F_π at the highest possible Q^2, and the additional studies needed to confirm its reliability, is thus 120 hours. About half of this time is invested in additional statistics for the highest Q^2 point and the rest is invested in validation studies.

It should also be noted that in comparison to what was planned for PAC35/38, the SHMS solid angle is now expected to be a bit smaller. This has resulted in an increase of beam time for some settings in comparison to PAC35/38, but this is offset by the savings produced by combining other settings.

V. PROJECTED RESULTS

To a good approximation in our kinematics, $\sigma_L \propto F_\pi^2$, so we need to first estimate the error on σ_L. A minimum of two measurements at fixed (Q^2, W) and different values of ϵ are needed in order to determine σ_L. Thus if $\sigma_1 = \sigma_T + \epsilon_1\sigma_L$ and $\sigma_2 = \sigma_T + \epsilon_2\sigma_L$ then

$$\sigma_L = \frac{1}{\epsilon_1 - \epsilon_2}(\sigma_1 - \sigma_2).$$

Assuming uncorrelated errors in the measurement of σ_1 and σ_2, we obtain the intermediate expression

$$\frac{\Delta\sigma_L}{\sigma_L} = \frac{1}{(\epsilon_1 - \epsilon_2)}\frac{1}{\sigma_L}\sqrt{\Delta\sigma_1^2 + \Delta\sigma_2^2},$$

and by defining $r \equiv \sigma_T/\sigma_L$

$$\frac{\Delta\sigma_L}{\sigma_L} = \frac{1}{\epsilon_1 - \epsilon_2}\sqrt{\left(\frac{\Delta\sigma_1}{\sigma_1}\right)^2(r+\epsilon_1)^2 + \left(\frac{\Delta\sigma_2}{\sigma_2}\right)^2(r+\epsilon_2)^2}.$$

This useful equation makes explicit the error amplification due to a limited ϵ range and (potentially) large r.

Again using the approximation that $\sigma_L \propto F_\pi^2$, the experimental error in F_π is

$$\frac{\Delta F_\pi}{F_\pi} = \frac{1}{2}\frac{1}{(\epsilon_1 - \epsilon_2)}\sqrt{\left(\frac{\Delta\sigma_1}{\sigma_1}\right)^2(r+\epsilon_1)^2 + \left(\frac{\Delta\sigma_2}{\sigma_2}\right)^2(r+\epsilon_2)^2}.$$

As far as the extraction of the form factor is concerned, the relevant quantities are $r = \sigma_T/\sigma_L$ and $\Delta\epsilon$ between the two kinematic settings.

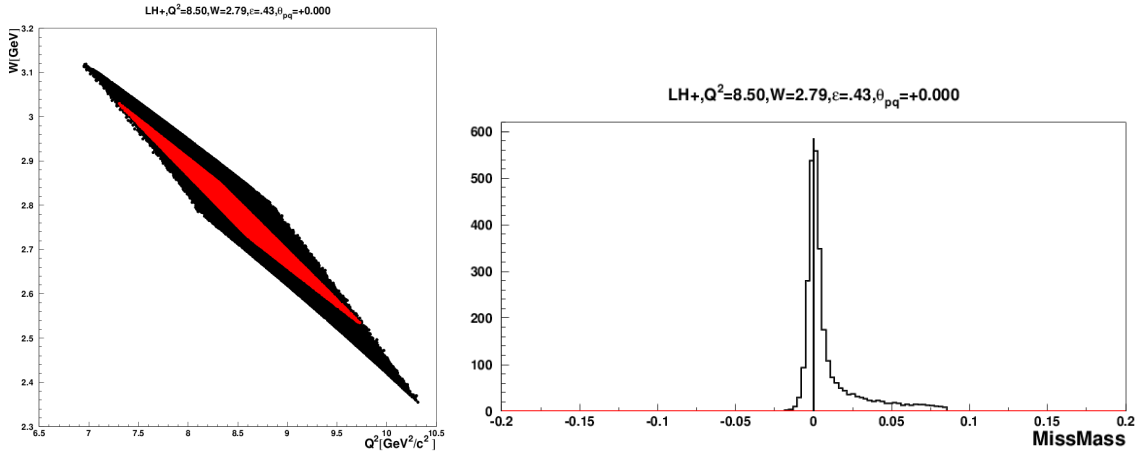

FIG. 5: *Left:* Simulated Q^2 (horizontal axis) versus W (vertical axis) acceptance for the Q^2=8.5 GeV^2 SHMS+HMS settings. The black points are the acceptance at ϵ =0.430, and the red points are the acceptance at ϵ =0.156. Cuts are applied to equalize the acceptances of the two settings. **Right:** Simulated $p(e,e'\pi^+)n$ missing mass distribution for the Q^2=8.5 GeV^2 $\epsilon = 0.43$ SHMS+HMS setting (the neutron mass is subtracted). The cutoff at right indicates the limit of the $0.875 < MM < 1.025$ GeV cut used for the rate estimates.

The error uncertainties for the Q^2=8.5 GeV^2 F_π extraction are projected using a Monte Carlo simulation of the SHMS+HMS setting, using the phenomenological model of Vrancx and Ryckebusch [18]. Nominal acceptance cuts of $|hsdelta| < 8\%$, $|hsxptar| < 0.08$, $|hsyptar| < 0.035$, $|ssdelta| < 15\%$, $|ssxptar| < 0.04$, $|ssyptar| < 0.024$ are applied. In addition, cuts are applied to equalize the SHMS+HMS acceptance at high and low ϵ and to select the exclusive neutron missing mass region (see Fig. 5). For the requested beam times listed in Table II, we estimate 14,000 good events per ϵ setting, divided unequally over 6 t-bins from $0.40 < -t < 1.00$ GeV^2(note that due to the finite acceptance of the HMS-SHMS system, $-t$ can be smaller than the value of $-t_{min}$ listed at the central kinematics is Table II). The statistical uncertainty per t-bin ranges from 1.6-3.6%, to which is added the estimated uncorrelated systematic error of 0.6%. Both of these are magnified by $1/\Delta\epsilon = 3.65$ in the L/T-separation.

TABLE V: Projected statistical and systematic uncertainties for $F_\pi(Q^2)$ assuming the VR model cross sections, the ϵ values and running times given in Tables I, II and the projected uncertainties given in the E12-06-101 proposal.

Q^2 (GeV^2)	$-t_{min}$ (GeV^2)	$r \equiv \sigma_T/\sigma_L$	$\Delta\epsilon$	$\Delta F_\pi/F_\pi$ (%)
E12-06-101				
0.30	0.005	0.68	0.406	4.9
1.60	0.029	0.36	0.409	4.1
2.45	0.048	0.37	0.326	4.6
3.85	0.120	0.55	0.365	4.7
5.00	0.209	0.78	0.395	5.0
6.00	0.212	0.70	0.268	6.1
Optimized E12-07-105				
8.50	0.544	1.71	0.274	10.2

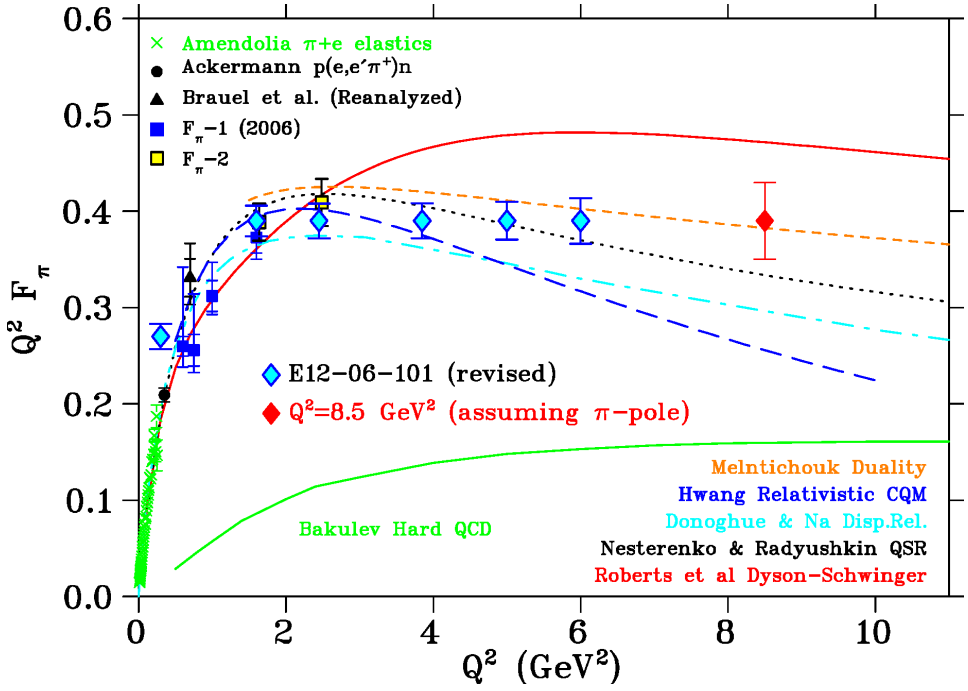

FIG. 6: Projected error bars for this SHMS+HMS proposal, in comparison with a variety of theoretical models, and existing precision data. The error bars include all projected statistical and systematic uncertainties.

The extraction of F_π from the data requires that the t dependence of $\sigma_{\rm L}$ be compared to the VGL Regge (or other) model. To estimate the uncertainty in F_π, we took into account both the variation of counts across the SHMS+HMS acceptance at both low and high ϵ and the variation in the VR model $r = \sigma_T/\sigma_L$ across the acceptance. This yields a projected statistical

and uncorrelated systematic uncertainty in F_π of 6.7%. However, the final uncertainty on F_π is also limited by the t-correlated uncertainty (1.6%), which is common to all t-bins at fixed ϵ but varies randomly between ϵ settings, and the overall scale uncertainty (3.3%). These additional errors yield a total projected uncertainty in F_π of 10.2%. This projection is sensitive to the assumption for the ratio $r = \sigma_T/\sigma_L$ (shown in Table V), which may be conservative.

The resulting projected error bars, including all statistical, systematic, and model fitting uncertainties, are listed in Table V and displayed in Fig. 6. We see that the proposed Q^2=8.5 GeV^2 measurement is easily able to distinguish between the models.

VI. SUMMARY

In summary, we request that the PAC confirm the high–impact status of the program we have described in this proposal and we request an additional 120 hours (5 days) to be used in conjunction with the time already approved for the E12-06-101 and E12-07-105 experiments. The combined beam time allocation will:

- enable measurements of the pion form factor at low $-t_{min}$ up to $Q^2 = 6$ GeV^2
- allow for measurements of the separated π^+ cross sections as a function of Q^2 at three fixed x values, and finally,
- enable the measurement of the pion form factor to the very largest Q^2 accessible at a 12 GeV JLab, 8.5 GeV^2.

Since this latter measurement will be at a value of $-t_{min}$ somewhat larger than that typically used for pion form factor measurements, some time will be used to provide experimental validation of the form factor extraction.

Taken together, this proposal combined with the already approved experiments will provide a comprehensive and coherent program of charged pion electroproduction, separated cross section measurements. Since there are strong theoretical grounds that hard contributions to the pion form factor dominate for $Q^2 \geq$8 GeV^2 [14], the proposed measurement will contribute greatly to our understanding of the pion form factor in the region where QCD begins to transition from large- to small-distance-scale behavior.

[1] T. Horn, C.D. Roberts, Journal of Physics G: Nuclear and Particle Physics, Vol. 43, Issue 7, 073001 (2016), arXiv:1602.04016.

[2] G.M. Huber, D.J. Gaskell, et al., Jefferson Lab Experiment E12-06-101, "Measurement of the Charged Pion Form Factor to High Q^2", http://www.jlab.org/exp_prog/proposals/06/PR12-06-101.pdf

[3] G.M. Huber, et al., Phys. Rev. C **91** (2015) 015202.
[4] L. Chang, C. Mezrag, H. Moutarde, C.D. Roberts, J. Rodrguez-Quintero, and P.C. Tandy, Phys. Lett **B737** (2014) 23.
[5] J. Segovia, L. Chang, I. Cloet, C.D. Roberts, S. Schmidt, and H.S. Zong, Phys. Lett **B731** (2014) 13.
[6] S. V. Goloskokov and P. Kroll, Eur. Phys. J. C **65**, 137 (2010); Eur. Phys. J. A **47**, 112 (2011).
[7] S. Ahmad, G.R. Goldstein, S. Liuti, Phys. Rev. D **79**, 054014 (2009); G.R. Goldstein, J.O.G. Hernandez, S. Liuti, J. Phys. G: Nucl. Part. Phys. **39**, 115001 (2012); G.R. Goldstein, J.O.G. Hernandez, S. Liuti, Phys. Rev. D **91**, 114013 (2015).
[8] T. Horn, G.M. Huber, et al., Jefferson Lab Experiment E12-07-105, "Scaling Study of the L-T Separated Pion Electroproduction Cross Section at 11 GeV", http://www.jlab.org/exp_prog/proposals/07/PR12-07-105.pdf
[9] C.E. Carlson, J. Milana, Phys. Rev. Lett. **65** (1990) 1717.
[10] C.J. Bebek, et al., Phys. Rev. D **17** (1978) 1693.
[11] T. Horn, et al., Phys. Rev. Lett. **97** (2006) 192001.
[12] G.M. Huber, et al., Phys. Rev. C **78** (2008) 045203.
[13] L. Chang, I.C. Cloet, J.J. Cobos-Martinez, C.D. Roberts, S.M. Schmidt, P.C. Tandy, Phys. Rev. Lett. **110** (2013) 132001.
[14] L. Chang, I.C. Cloet, C.D. Roberts, S.M. Schmidt, P.C. Tandy, Phys. Rev. Lett. **111** (2013) 141802.
[15] Department of Energy, Nuclear Science Advisory Committee, "Reaching for the Horizon" Long Range Plan (2015), Available online: http://science.energy.gov/~/media/np/nsac/pdf/2015LRP/2015_LRPNS_091815.pdf.
[16] P. Brauel, et al., Z. Phys. C **3** (1979) 101.
[17] M. Vanderhaeghen, M. Guidal, J.-M. Laget, Phys. Rev. C **57** (1997) 1454.
M. Vanderhaeghen, M. Guidal, J.-M. Laget, Nucl. Phys. **A627** (1997) 645.
[18] T. Vrancx, J. Ryckebusch, Phys. Rev. C **89**, 025203 (2014).
[19] Report of the Jefferson Lab Program Advisory Committee - PAC30 (2006), Available online: https://www.jlab.org/exp_prog/PACpage/PAC30/PAC30_report.pdf
[20] Report of the Jefferson Lab Program Advisory Committee - PAC32 (2007), Available online: https://www.jlab.org/exp_prog/PACpage/PAC32/PAC32_report.pdf

APPENDIX A: SHMS OPTICS STUDIES

The original versions of the E12-06-101 and E12-07-105 proposals assumed an 8 cm cryotarget length in order to minimize uncertainties introduced from the change in extended target acceptance between large and small electron spectrometer (HMS) angles. The SHMS has very large and uniform y_{target} acceptance, and is used primarily at forward angles, so the extended target acceptance is not a concern for the pion arm.

We have examined the impact of using a slightly longer target (10 cm), which would allow the use of correspondingly lower beam currents. Figure 7 shows the extended target acceptance in the HMS at relatively small angles (20 degrees) and at the largest angle that would be used

in this experiment, 57.7 degrees. The acceptance is plotted as the effective solid angle (for a given HMS δ range) vs. z along the target. As can be seen in the figure, the acceptance is the same at $z = 0$, but drops slightly faster at larger values of $|z|$ for the 57.7 degree case. At the edges of the target ($z = \pm 5$ cm) the acceptance drops by about 25% overall for the large angle case, or about 15% as compared to the small angle case. Simulation indicates that most of the "extra" lost events occur due to apertures in the first two HMS quadrupole magnets.

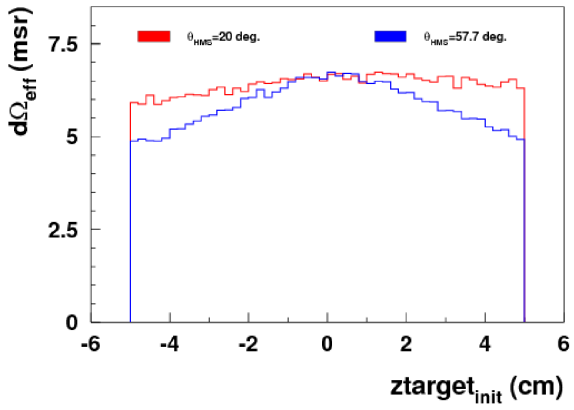

FIG. 7: Simulated acceptance of the HMS for long (10 cm) targets at small (20 degrees) and large (57.7 degrees) angles. The red curve shows the effective solid angle as a function of z_{target} for an HMS angle of 20 degrees and the blue curve for 57.7 degrees. At small angles the variation in the acceptance for extended targets results in a change of 10% and at large angles of about 25%.

While some care must be taken to ensure that the change in acceptance is well understood, since the differences are rather modest the problem is a tractable one. The most straightforward way to verify our understanding of the extended target acceptance is to take inclusive electron scattering data in the DIS region, from thin targets positioned at the extremes (and at the center) of the spectrometer y_{target} acceptance. Verification that the same DIS cross section is extracted independent of y_{target} will guarantee that the extended target acceptance is well understood, and that there will be minimal or no impact on the point-to-point uncertainties in this experiment.

There will be some studies of the extended target acceptance of the HMS at large angles performed as part of the re-commisioning of the Hall C apparatus (via comparison of cross sections from 4 cm and 10 cm cryotargets as well as point target studies). If more data are required for the F_π measurements, the inclusive DIS study described above can readily be accomplished in about 8 hours of beam time.